

Influence of nanopowder characteristics on dispersion property of slurries

Jinyi Choi^a, Younggeul Jung^a, Jeonghee Kim^a, Dongwook Shin^{a,b,*}

^aDepartment of Fuel Cells and Hydrogen Technology, Hanyang University, Seoul 133-791, Republic of Korea

^bDivision of Materials Science & Engineering, Hanyang University, Seoul 133-791, Republic of Korea

Available online 30 October 2012

Abstract

To investigate the effect of nanopowder characteristics on the slurry properties, the comparative studies on three types of SDC nanopowder synthesized by different methods, i.e., hydrothermal (commercial, SDC I), sol–gel (commercial, SDC II) and citric-nitrate combustion (lab-made, SDC III), were carried out. The powder properties were investigated using X-ray diffraction, BET surface area and laser particle size analysis. The slurry stability was confirmed by zeta potential and sedimentation experiments. The samples were similar in the powder sizes, shapes and agglomeration degrees. However, when these samples were dispersed into slurry, the deagglomeration behaviours of particles and dispersion stabilities were significantly different. The powders consist of agglomerates with the average sizes of about 5 µm; these agglomerates were primary composed of particles with the average size of 20–30 nm. After dispersion, the agglomerates sizes of SDC I, II, and III were reduced to 454.7, 120.5, and 54.8 nm, respectively. The slurry of lab-made SDC nanopowders was the most stable, which resulted from soft agglomeration originated from the nature of synthesis process.

© 2012 Elsevier Ltd and Techna Group S.r.l. All rights reserved.

Keywords: A. Suspensions; D. CeO₂; E. Fuel cells

1. Introduction

A ceria-based material doped with gadolinia, samaria, and yttria (as GDC, SDC, and YDC) has been regarded as one of the key materials for solid oxide fuel cells (SOFCs), especially for the electrolyte in intermediate temperature SOFCs and the barrier layer on yttria-stabilized zirconia (YSZ) electrolyte. In practical application of these functions, thin-film type configuration is essential to reduce the operation temperature below 650 °C or for conformal coating of barrier (buffer) layer on irregular surfaces.

The feasibility of the wet powder spraying (WPS), an easy and low-cost technique applicable to the planar or tubular substrates for thin film deposition of the electrolyte has been widely demonstrated or SOFCs application [1,2]. In order to obtain a thin and uniform film using WPS technique, there

are two essential components to secure: (i) the nanopowder with the narrow size distribution and homogeneous particle morphology to reduce microstructural defects in the sintered film [3,4] and (ii) the slurry with high dispersion stability to prevent the agglomerates in the slurry resulting in lower packing density and significant residual porosity [5,6].

Recently, wet chemical synthesis methods such as sol–gel [7] and hydrothermal [8] have been developed to produce the homogeneous and fine ceria nanopowders. However, the sophisticated controls of the process parameters in the WPS process have been hampered by unpredictable dispersion behaviors of the nanopowders in the slurry even though those have similar physical powder characteristics such as particle size/distribution and the degree of agglomeration. Therefore, it would be worth contemplating the surface chemical characteristics of the powders, which are mainly originated from the synthesis method.

The aim of this work is to investigate the influence of the nanopowder synthesis method on the dispersion properties of slurry. The comparison of the dispersion properties of nanopowders synthesized by various methods is a complicated work since each process has its own optimized conditions in

*Corresponding author at: Hanyang University, Department of Fuel Cells and Hydrogen Technology, Seoul 133-791, Republic of Korea. Tel.: +82 2 2220 0503; fax: +82 2 2220 4011.

E-mail address: dwshin@hanyang.ac.kr (D. Shin).

numerous process parameters and it is almost impossible to maintain constant experimental condition throughout these various methods. Thus, in the present work the physical parameters such as particle size and the degree of agglomeration are fixed for the rigorous analysis of dispersion characteristics and their origins. To realize these experimental conditions, the powders having similar particle size were selected regardless of detailed synthesis conditions.

2. Experimental

2.1. Samples preparation

Commercial nano-SDC powders obtained via hydrothermal synthesis (NexTech Materials, USA) and sol–gel method (NaBond technology Co. Ltd., China) were referred to as SDC I and SDC II, respectively.

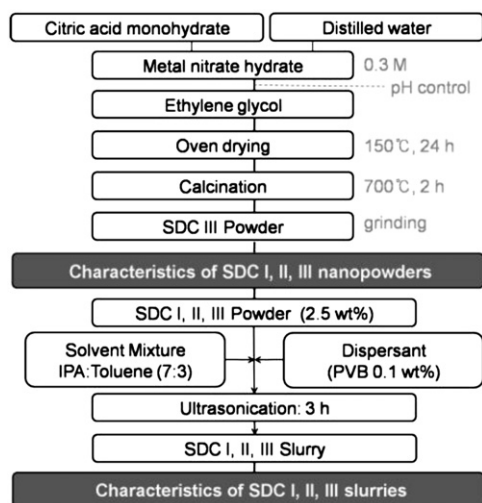


Fig. 1. Experimental flow chart.

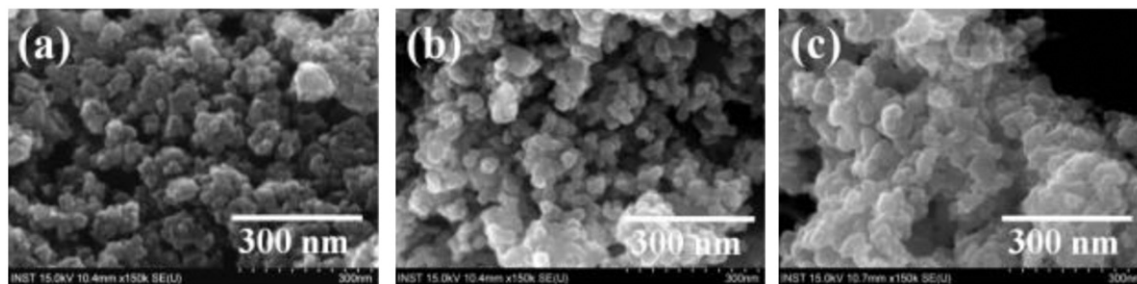


Fig. 2. Powders morphologies of (a) SDC I, (b) SDC II, and (c) SDC III.

SDC III powders prepared by the citric-nitrate combustion process $\text{Ce}(\text{NO}_3)_3 \cdot 6\text{H}_2\text{O}$ [Sigma-Aldrich > 99.9%] and $\text{Sm}(\text{NO}_3)_3 \cdot 6\text{H}_2\text{O}$ [Sigma-Aldrich, 99%] were used as the starting materials. Stoichiometric amounts of 0.3 M metal salts were dissolved in distilled water. Citric acid monohydrate ($\text{C}_6\text{H}_8\text{O}_7 \cdot \text{H}_2\text{O}$, purity > 99.0%) was added to the above nitrate solutions and the molar ratio of metal to citric acid was set to 5:1. The solution was evaporated at 80 °C to form a transparent gel. After drying at 150 °C for 24 h, the transparent gel changed to a brown dry gel. The dry gel was subsequently fired at 700 °C for 2 h to obtain the nano-SDC (SDC III).

The SDC I, II, III slurries were prepared by mixing individual powders and bi-solvent with polyvinyl butyral (PVB) and were sonicated for 3 h to break up the agglomerated particles.

2.2. Samples characterization

Field-emission scanning electron microscopy (S-4800, HITACHI), BET surface area measurement (ASAP 2020, Micromeritics), X-ray diffractometer (ULTIMA IV, Rigaku) and Laser particle size analyzer (LPA-3000, 3100, Otsuka electronics) were used to characterize SDC nanopowders prior to prepare slurries. Also, three types of slurries were characterized by zeta-potential (Zetasizer 300HS, Malvern Instruments Ltd.) and turbiscan (Turbiscan Lab Expert, Formulaction) Fig. 1.

3. Results and discussion

3.1. Characteristics of the SDC nanopowders

Fig. 2 shows SEM micrographs of the three different powders described in Table 1. Although calcination

Table 1
The powder properties of three types of specimen used in the study.

Sample	Particle shape	BET (m ² /g)	D_{BET} (nm)	Particle size distribution (nm)		
				D10	D50	D90
SDC I (Hydrothermal, commercial)	Spherical	185	4.6	855	5508	17740
SDC II (Sol–gel, commercial)		70	12.0	793	4005	13470
SDC III (Citric-nitrate, lab-made)		30	28.0	831	4403	10210

temperatures may be different, it is clear that all the samples have approximately same particle size and shape regardless of preparation method. The shapes of the samples were nearly spherical and the size of the particles ranged from 20 to 30 nm. Among the samples, SDC I is slightly smaller compared to the other samples.

As shown in Fig. 3, the XRD pattern of the lab made SDC III exhibited that of the fluorite-type structure with cubic lattice symmetry with high crystallinity. In addition, the XRD peaks for the SDC I are noticeably broadened and the other powders are also similar in this aspect. BET measurement reveals that particles are aggregates of many small primary crystallites with the diameters of 4–30 nm (from BET data in Table 1, D_{BET}). The calculation from the peak broadening shows that the crystallite sizes of SDC I, II, and III were 3.98, 10.24, and 20.24 nm, which are in agreement with the BET results summarized in Table 1. XRD and BET results show that commercial hydrothermally synthesized SDC I nanopowder has relatively smaller grain size than sol–gel synthesized SDC II and citric nitrate synthesized SDC III. Therefore, it is clear that the crystallite size and the degree of agglomeration are strongly determined by the nature of powder synthesis technique.

In order to analyze the agglomeration state, the results of particle-size distribution of three powders in ethanol media are compared in Fig. 4 and Table 1. After 10 min of ultrasonic agitation, all samples presented an almost

similar size range, which reveals that there is a similar tendency in agglomeration behaviour. The SDC III nanopowder showed relatively narrower size distribution and smaller aggregate size.

3.2. Characteristics of the SDC slurries

The aforementioned results confirm that the samples synthesized by different method are similar in size, shape and the degree of agglomeration except primary crystallite size. To characterize the dispersion of slurries, the results of zeta potential measurements on diluted slurry of the three types of nanopowders are summarized in Table 2.

A higher zeta potential value means higher repulsive forces between particles and consequently higher slurry stability. The result indicates that SDC III slurry has sufficient surface charge ensuring high dispersion stability.

The particle size distributions of slurries were also measured by zeta-sizer. In contrast to that of raw powders (Fig. 4), Table 2 and Fig. 5 show remarkable differences in the average size and the distribution of particles when dispersed in the slurries. As a result of the dispersant and the sonication process to obtain the homogeneous slurry, the average particle size of SDC I, II and III were reduced from 5508, 4005 and 4403 nm to 454.7, 120.5 and 54.8 nm, respectively. The SDC III slurry shows the narrower distribution and smaller aggregate size (54.8 nm), suggesting that this slurry is easy to deagglomerate by dispersing agent or mechanical dispersion. SDC I nanopowder slurry shows bimodal distribution and large aggregate size (454.7 nm) caused by hard agglomeration effect.

Sedimentation behaviours of slurries containing the SDC nanopowders are compared in Fig. 6. The transmitted light intensity is inversely proportional to the degree of sedimentation. As the sedimentation of particles proceeds, the transmission light intensity of the upper part of the glass vial will become higher. After 20 h, the transmission increases in the

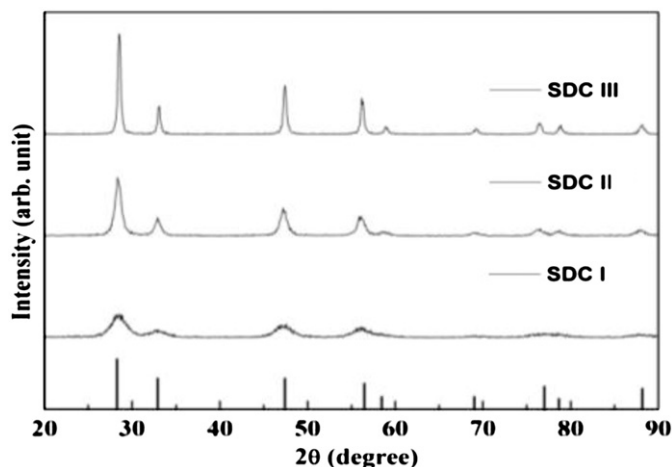


Fig. 3. X-ray diffraction patterns of the powders: (a) SDC I, (b) SDC II, and (c) SDC III.

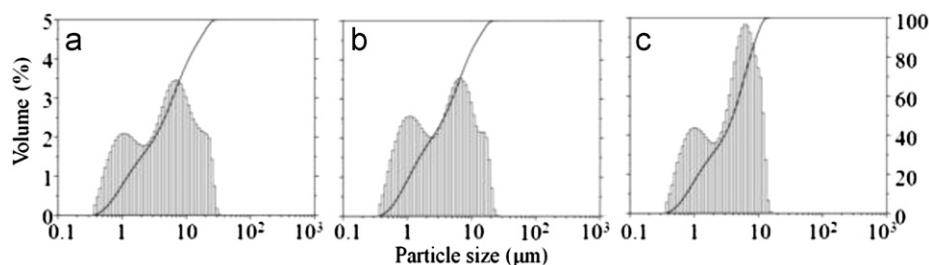


Fig. 4. Particle-size distribution of the powders: (a) SDC I, (b) SDC II, and (c) SDC III.

Table 2

Dispersion parameters of slurries evaluated by zeta-sizer.

Properties	SDC I	SDC II	SDC III
Zeta potential (mV)	28.96	20.55	45.96
$D_{\text{Zeta-Sizer}}$ (nm)	454.7	120.5	54.8

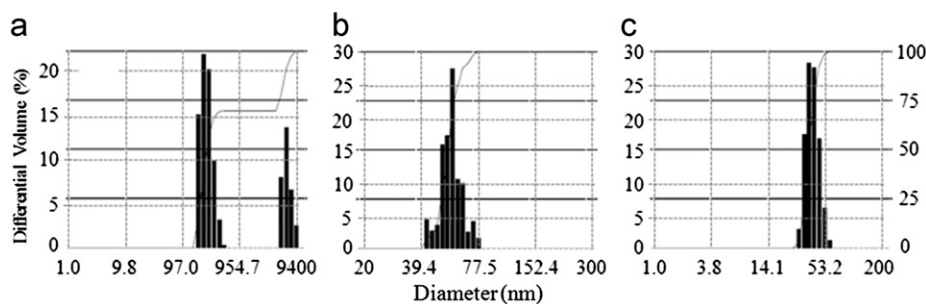


Fig. 5. Size distribution of the particles dispersed in slurry: (a) SDC I, (b) SDC II, and (c) SDC III.

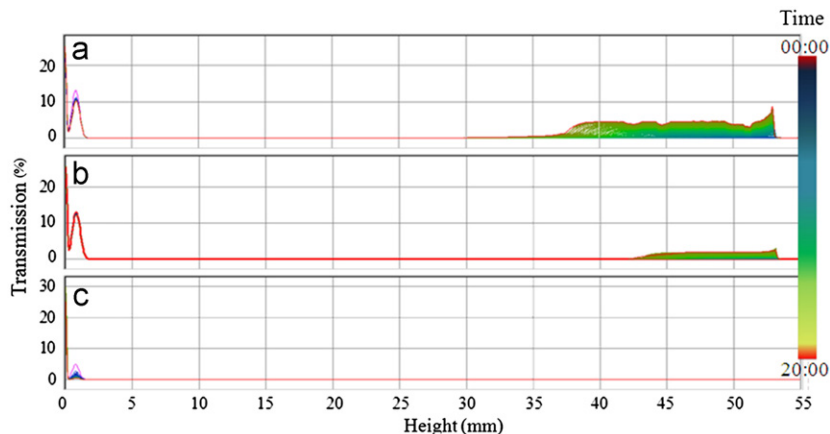


Fig. 6. Transmission scanning with time for (a) SDC I, (b) SDC II, and (c) SDC III.

upper part due to the clarification of SDC I slurry is significant compared to the other samples. This means that the sedimentation was accelerated by the agglomerated particles in the specimen prepared by hydrothermal method with time. However, SDC III slurry shows no clarification and small particles are well dispersed in the slurry even after long time. It is clear from the previous results that this is due to the difference in the degree of agglomeration of the particles in the nanopowders. The nanopowders prepared by wet chemical synthesis methods using aqueous solution have a hard agglomeration between the particles since the surface hydroxide structures of Adjacent particles could bridge by creating crystalline structures [9]. Although the SDC III was also prepared by citric-nitrate combustion which belongs to wet chemical synthesis methods using aqueous solution, the agglomeration in this slurry is significantly lower as much as initial particle size, and this maintained even after dispersion in the solvent. This result indicates that the amount of molecular H_2O surrounding the as-prepared powder plays an important role in determining the hard agglomeration in wet chemical synthesis methods using aqueous solution [10]. In general, hydrothermal and sol-gel method involves the washing process and there is no steps to break the aforementioned particle bridging by hydrogen bonding. However, in case of citric-nitrate combustion, the heat generated by exothermic reaction during fuel and nitrate decomposition and large gas release [11] might be sufficient to break the hydrogen bonding and prevent the hard agglomerate formation of nanopowders.

From the experimental results, one can conclude that in thin film deposition by WPS using the slurry it should be considered not only the final particle size or crystallite size but also the selection of synthesis route.

4. Conclusions

Three different SDC nanopowders were characterized and prepared into slurries to study nanopowder dispersion stability which is essential to fabricate ceramic thin films by wet powder processing. It is shown that citric nitrate combustion synthesized lab-made SDC III nanopowder slurry leads to less aggregation and higher dispersion stability in IPA:Toluene (7:3) dispersion medium with PVB as a dispersant than hydrothermal synthesized SDC I and sol-gel synthesized SDC II nanopowder slurries, though the primary crystallite size of the SDC III nanopowder is larger than the others. This is a result from soft agglomeration caused by a citric-nitrate combustion effect during the synthesis process. In conclusion, to achieve highly dispersed nanopowder slurries, it is necessary to take into consideration of not only basic nanopowder characteristics but also the selection of synthesis route which prevents the hard agglomeration. The effect of powder characteristics include its specific synthesis route on dispersion state requires further study.

Acknowledgements

This work is the outcome of a Manpower Development Program for Energy supported by the Ministry of Knowledge and Economy (MKE), and also supported by Solid oxide fuel cell of New & Renewable Energy R&D program (20093021030010) under the Korea Ministry of Knowledge Economy (MKE).

References

- [1] E. Schüller, R. Vaßen, D. Stöver, Thin electrolyte layers for SOFC via wet powder spraying (WPS), *Advanced Engineering Materials* 4 (2002) 659–662.
- [2] W. Zhou, H. Shi, R. Ran, R. Cai, Z. Shao, W. Jin, Fabrication of an anode-supported yttria-stabilized zirconia thin film for solid-oxide fuel cells via wet powder spraying, *Journal of Power Sources* 184 (2008) 229–237.
- [3] W.H. Rhodes, Agglomerate and particle size effect on sintering yttria-stabilized zirconia, *Journal of the American Ceramic Society* 64 (1981) 19–22.
- [4] P. Duran, M. Villegas, F. Capel, C. Moure, Low-temperature fully densified nanostructured Y-TZP ceramic, *Journal of Material Sciences* 15 (1996) 741–744.
- [5] L. Günther, W. Peukert, Control of coating properties by tailored particle interactions: relation between suspension rheology and film structure, *Colloids and Surfaces A* 225 (2003) 49–61.
- [6] W.J. Tseng, C. Wu, Sedimentation, rheology and particle-packing structure of aqueous Al_2O_3 suspensions, *Ceramics International* 29 (2003) 821–828.
- [7] Y. Tao, J. Shao, J. Wang, W. Wang, Morphology control of $\text{Ce}_{0.9}\text{Gd}_{0.1}\text{O}_{1.95}$ nanopowder synthesized by sol–gel method using PVP as a surfactant, *Journal of Alloys and Compounds* 484 (2009) 729–733.
- [8] M. Cheng, D. Hwang, H. Sheu, B. Hwang, Formation of $\text{Ce}_{0.8}\text{Sm}_{0.2}\text{O}_{1.9}$ nanoparticles by urea-based low-temperature hydrothermal process, *Journal of Power Sources* 175 (2008) 137–144.
- [9] M.S. Kaliszewski, A.H. Heuer, Alcohol Interaction with Zirconia Powders, *Journal of the American Ceramic Society* 73 (1990) 1504–1509.
- [10] G.B. Jung, T.J. Huang, Preparation of samaria-doped ceria for solid-oxide fuel cell electrolyte by a modified sol–gel method, *Journal of Material Sciences* 36 (2001) 5839–5844.
- [11] K. Zupan, D. Kolar, M. Marinšek, Influence of citrate–nitrate reaction mixture packing on ceramic powder properties, *Journal of Power Sources* 86 (2000) 417–422.